Preparation and Properties of Nylon-1010/Montmorillonite Nanocomposites by Melt Intercalation

Zengjun Liu, Peilin Zhou, Deyue Yan

College of Chemistry and Chemical Technology, Shanghai Jiao Tong University, 800 Dongchuan Road, Shanghai 200240, China

Received 23 September 2002; accepted 28 May 2003

ABSTRACT: Two types of nylon-1010/MMT nanocomposites were successfully prepared by melt intercalation using a corotating twin-screw extruder. The nanocomposites were characterized with X-ray diffraction (XRD), scanning electron microscopy, transmission electron microscopy (TEM), thermogravimetric analysis, differential scanning calorimetry, and dynamic mechanical analysis (DMA). It was found that the difference in the properties of the two types of the organo-MMTs directly influences the structure and the properties of the obtained nanocomposites. The results of XRD and TEM showed that the DK2-MMT nanocomposites possess an exfoliated structure and the nanocomposites containing 16C-MMT exist as intercalated structures. The mechanical properties of the nylon-1010/organo-MMTs nanocomposites were better than those of the pure nynon-1010. In addition, the properties of the DK2-MMT nanocomposites were superior to those of the 16C-MMT nanocomposites because of the different dispersibility of the two organo-MMTs. The thermal stability of the nanocomposites was improved. The storage moduli of the nanocomposites increased and the glass-transition temperature shifted to a slightly higher temperature because of the introduction of the organo-MMTs. The addition of DK2-MMT into the nylon-1010 matrix accelerated the crystallization rate of the matrix. © 2003 Wiley Periodicals, Inc. J Appl Polym Sci 91: 1834–1841, 2004

Key words: nylon-1010; montmorillonite; nanocomposites; melt intercalation; mechanical properties

INTRODUCTION

Improving the mechanical properties of existing polymers is an ongoing goal of polymer scientists. In the past decades, investigators usually adopted the methods of polymer blending and inorganic mass filling to improve the properties of polymers. Recently, another technology—the compounding of the polymers with clay at the nanoscale level—has attracted great interest of polymer scientists since the Toyota research center[1,2] first reported the polyamide 6/clay nanocomposite. Up to now, many polymers have been used to synthesize polymer/clay nanocomposites successfully.[3–18] These polymer/clay nanocomposites (PCNs) frequently exhibit excellent physical and mechanical properties with typical filler amounts of less than 5 wt %, such as improved strength, enhanced modulus, decreased thermal expansion coefficients, increased thermal stability, and reduced gas permeability, compared to those of pure polymers or conventional composites, attributed to the nanoscale dispersion of clay in the polymer matrix, high aspect ratio of clay platelets, and interfacial interaction between clay and polymers.

As a component of PCN, the commonly used clay is montmorillonite (MMT) because of its natural abundance and low cost. MMT has a typical 2 : 1 layered structure, which consists of two silica tetrahedral sheets fused to one alumina octahedral sheet. The individual MMT layer is about 1 nm thick. Thus, PCN can be obtained if only MMT layers uniformly disperse in the polymer matrix. In general, there are three methods to obtain PCN: (1) solution intercalation; (2) *in situ* intercalative polymerization; and (3) melt intercalation. Compared with the first and the second methods, melt intercalation has the advantages of being environmentally benign because of the absence of solvent and of using conventional extrusion equipments for preparation. Therefore, melt intercalation is one of the promising ways of preparing thermoplastic PCN.

When nanolayers of MMT are dispersed in the polymer matrix, two types of nanocomposites can be obtained. Intercalated nanocomposites are formed when a few polymer chains are located between the MMT layers but regularly spaced stacks of MMT layers are maintained. An exfoliated or delaminated structure is formed when MMT layers are uniformly dispersed throughout the whole polymer matrix.

Correspondence to: D. Yan (dyyan@mail.sjtu.edu.cn).

Contract grant sponsor: Ministry of Science and Technology of China; contract grant number: 973 Project G1999064802.

Journal of Applied Polymer Science, Vol. 91, 1834–1841 (2004)

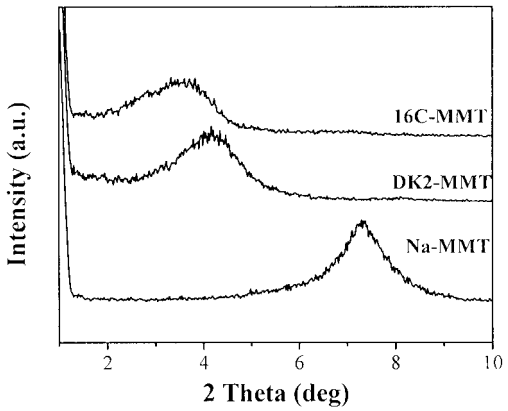

Figure 1 XRD patterns of Na-MMT, DK2-MMT, and 16C-MMT.

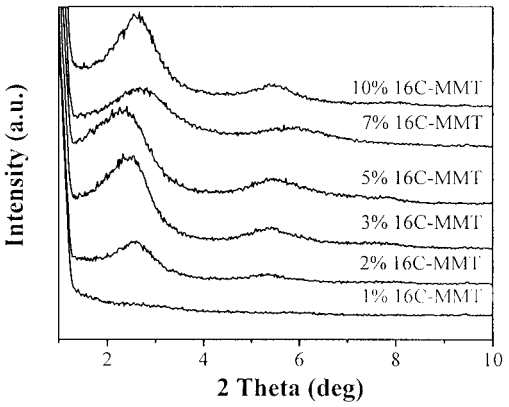

Figure 3 XRD patterns of the 16C-MMT nanocomposites with different 16C-MMT contents.

Poly(decamethylene sebacamide) (nylon-1010) is a kind of engineering plastic developed and industrialized in China, which is usually used to manufacture exact parts, meters, and home appliances. Its dimensional stability and impact strength are superior, although its strength and modulus are inferior, to those of nylon-6 and nylon-66. Although compounding with clay in nanoscale is an effective way to improve strength and modulus of polymers, until now there have been no reports on nylon-1010/clay nanocomposites. In this study, we prepared two types of nylon-1010/MMT nanocomposites by melt intercalation using a corotating twin-screw extruder and investigated the effect of different MMT contents on the structure and mechanical properties of the nylon-1010/MMT nanocomposites.

EXPERIMENTAL

Materials

Nylon-1010 used in this study is a commercially available material produced by Shanghai Cellulose Factory with the number-average molecular weight of about 20,000. Sodium montmorillonite (Na-MMT) and DK2 montmorillonte (DK2-MMT) were supplied by Zhejiang FengHong Clay Co. (China), both of which have a cation-exchange capacity of 120 meq/100 g and a particle size of <50 μm. DK2-MMT, a kind of organoclay, was modified with methyl tallow bis(2-hydroxyethyl) ammonium cations.

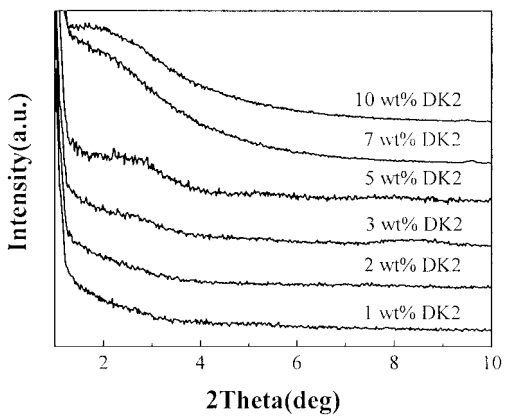

Figure 2 XRD patterns of the DK2-MMT nanocomposites with various DK2-MMT contents.

Preparation of 16C-MMT

The 16C-MMT was prepared by ion-exchange reaction. A water solution of 13.1 g hexadecyl trimethylammonium chloride was added to a 20 g Na-MMT suspension. The mixture was stirred vigorously for 1.0 h at 80°C and then filtered to obtain a white precipitate. The precipitate was washed repeatedly with hot water until no Cl^- was detected by adding 0.1 mol/L $AgNO_3$ solution. The product was then dried in a vacuum oven at 80°C to a constant weight and ground into a particle size of <50 μm.

Preparation of nylon-1010/MMT nanocomposites

Before preparation, samples of nylon-1010 were dried in a vacuum oven for 12 h at 100°C to avoid moisture-induced degradation reactions. All nanocomposites were prepared by melt-compounding of nylon-1010 and two kinds of organo-montmorillonite (organo-MMTs) using a corotating twin-screw extruder with screws of 35 mm diameter and L/D = 48, respectively. The barrel temperature was 210–235°C and the screw speed was 120 rpm.

Characterization

X-ray diffraction (XRD) patterns were recorded using a Rigaku III Dmax 2500 diffractometer (Rigaku, Japan) equipped with Ni-filtered Cu–K_α radiation (λ = 1.54

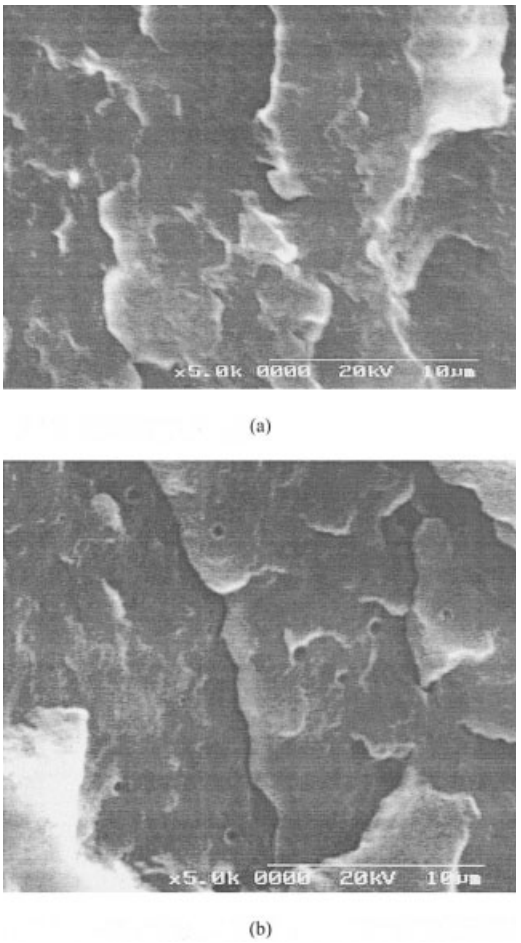

Figure 4 SEM micrographs of the nanocomposites containing 3 wt % organo-MMTs: (a) DK2-MMT and (b) 16C-MMT.

Å). The voltage and current of the X-ray tubes were 40 kV and 30 mA, respectively; corresponding data were collected from 1.0 to 30° at a scanning rate of 4°/min with a step size of 0.02°.

The morphology of the freeze-fractured surfaces of the samples was investigated using a Hitachi S-2150 scanning electron microscope (SEM; Hitachi, Ibaraki, Japan) using an acceleration of 20 kV. The samples were sputter-coated with gold for enhanced conductivity. Images were displayed on the monitor and directly saved in the computer connected with SEM.

Transmission electron micrographs (TEM) were obtained on a Philips CM120 transmission electron microscope (Philips, The Netherlands) using an acceleration voltage of 75 kV. Ultrathin sections (~ 100 nm thick) were cut with a Reichert-Jung Ultracut E microtome (Leica, Germany) equipped with a diamond knife and placed in a 200-mesh copper grid.

Thermogravimetric analysis (TGA) was carried out on a Perkin–Elmer TGA 7 thermogravimetric analyzer (Perkin Elmer Cetus Instruments, Norwalk, CT). The temperature range was from 50 to 700°C at a heating rate of 20°C/min under air atmosphere.

The dynamic mechanical properties of the pure nylon-1010 and nylon-1010/MMT nanocomposites films were measured with a TA 2980 dynamic mechanical analyzer (DMA; TA Instruments, New Castle, DE)). The analyzer was operated at 1 Hz, at a heating rate of 5°C/min under nitrogen atmosphere.

Differential scanning calorimetry (DSC) was performed on Perkin–Elmer Pyris-1. All DSC measurements were carried out under nitrogen atmosphere and samples were round sheets of 2.9–3.1 mg. Isothermal crystallization were carried out by heating the sample to 230°C and keeping for 10 min to eliminate thermal history, then cooling the sample to the predetermined temperature at a cooling rate of 200°C/min; the exothermic crystallization peak was recorded as a function of time.

Tensile strength was measured according to ASTM D638 at a crosshead speed of 50 mm/min using an Instron model 4465 testing machine. The flexural strength was obtained according to ASTM D790 at a crosshead speed of 1.3 mm/min using the same machine. Notched Izod impact tests were performed according to ASTM D256 using Ray-Ran testing equipment (UK). All the values reported are an average of at least five measurements.

RESULTS AND DISCUSSION

Dispersibility of the organo-MMTs in nylon-1010

Figure 1 shows XRD patterns of Na-MMT, DK2-MMT, and 16C-MMT. Pristine Na-MMT shows a strong diffraction peak at $2\theta = 7.30°$, corresponding to the (001)

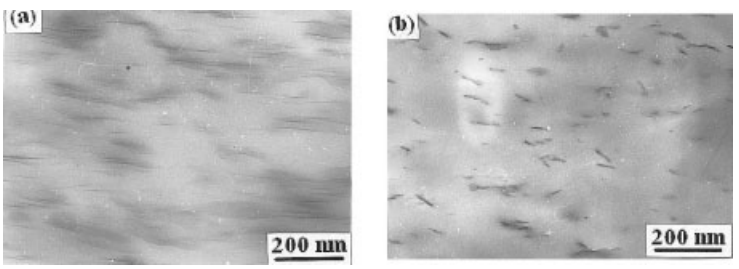

Figure 5 TEM micrographs of the nanocomposites containing 3 wt % organo-MMTs: (a) DK2-MMT and (b) 16C-MMT.

TABLE I
Mechanical Properties of Nylon-1010 and the Nanocomposites

Sample	MMT content (wt %)	Notched Izod impact strength (J/m)	Tensile strength (MPa)	Tensile modulus (GPa)	Flexural strength (MPa)	Flexural modulus (GPa)
Nylon-1010	0	38	43.4	1.44	56.1	1.20
DK2-MMT	1	42	46.6	1.60	63.6	1.41
	2	38	48.6	1.82	66.6	1.53
	3	38	52.1	1.97	71.1	1.69
	5	35	53.0	2.08	71.9	1.85
	7	31	54.2	2.21	73.1	2.04
	10	25	54.4	2.36	73.6	2.24
16C-MMT	1	36	48.2	1.51	60.7	1.41
	2	33	47.7	1.52	61.9	1.40
	3	27	48.6	1.57	62.3	1.48
	5	25	50.6	2.10	65.4	1.66
	7	24	50.5	2.18	67.5	1.85
	10	24	50.5	2.28	68.1	1.97

plane. According to Bragg's equation $2d \sin \theta = n\lambda$, the basal spacing is equal to 12.1 Å. The (001) plane diffraction peaks of DK2-MMT and 16C-MMT decrease to 4.10 and 3.57°, which correspond to the basal spacing of 21.5 and 24.7 Å, respectively. The XRD results imply, because of bigger size of the two kinds of organophilic modifiers compared with inorganic Na^+, that the organo-MMTs were swollen and had larger interlayer spacing than that of pristine Na-MMT. The increase of interlayer spacing and the change of interlayer microenvironment facilitate the intercalation of polymer chains into organo-MMT interlayers.

XRD patterns of the nylon-1010/DK2-MMT nanocomposites are presented in Figure 2. In Figure 2, no diffraction reflections can be observed in $2\theta \leq 10°$ for the DK2-MMT nanocomposites with 1–3 wt % DK2-MMT. It means that the ordered structure of DK2-MMT was destroyed and DK2-MMT layers exfoliated in the nylon-1010 matrix. When the DK2-MMT content is above 3 wt %, the existence of extremely weak peaks in the XRD patterns indicates that a small fraction of DK2-MMT is not delaminated and forms the partially exfoliated nanocomposites. Figure 3 shows XRD patterns of the 16C-MMT nanocomposites. The diffraction peaks of the remaining 16C-MMT nanocomposites appear at a lower degree compared with that of 16C-MMT except for the 16C-MMT nanocomposite containing 1 wt % 16C-MMT, implying the intercalated structure of these 16C-MMT nanocomposites. As for the 16C-MMT nanocomposite with 1 wt % 16C-MMT, no diffraction peak can be detected. There are two possibilities for this phenomenon: (1) the 16C-MMT (1 wt %) nanocomposite forms a highly exfoliated structure; (2) the content of 16C-MMT is too low to be detected by the X-ray diffractometer used. Under the same processing conditions, the compounding of DK2-MMT with the nylon-1010 is prone to the formation of an exfoliated structure and the melt blending of 16C-MMT with the nylon-1010 tends toward intercalated nanocomposites. Here, the interaction between organo-modifiers and polymer chains plays an important role in dependency on the structure of the obtained nanocomposites. In this study, DK2-MMT was modified with methyl tallow bis(2-hydroxyethyl) ammonium and the strong dipole–dipole interaction between the nylon-1010 matrix and the strongly polar hydroxyl groups of the modifier is the driving force of the nylon-1010 chains into the DK-MMT galleries. Therefore, the DK2-MMT nanocomposites form an exfoliated structure. However, alkyl groups of the modifier of 16C-MMT are nonpolar and weakly interact with the nylon-1010; thus the intercalated 16C-MMT nanocomposites were obtained.

Morphology of the nanocomposites

SEM micrographs of the nylon-1010 nanocomposites containing different 3 wt % organo-MMTs are compared in Figure 4. No particles can be observed on the fracture surface of the DK2-MMT nanocomposite [Fig. 4 (a)], suggesting good dispersion of DK2-MMT in the nylon-1010 matrix and no aggregation. However, a few 16C-MMT aggregates with a size of about 400–600 nm appear in the image of the 16C-MMT nanocomposite [Fig. 4 (b)]. The result of comparison means that DK2-MMT has better dispersion than that of 16C-MMT and organo-modification of DK2-MMT is more efficient than that of 16C-MMT.

TEM is a powerful tool that provides direct evidence of nanoscale dispersion of organo-MMTs in the polymer matrix. Figure 5(a) and (b) show TEM micrographs of the nylon-1010 nanocomposites containing different 3 wt % organo-MMTs. The dark lines in Figure 5(a) represent intersections of DK2-MMT sheets, whereas the gray part represents the nylon-1010 matrix. It can be seen that the DK2-MMT sheets

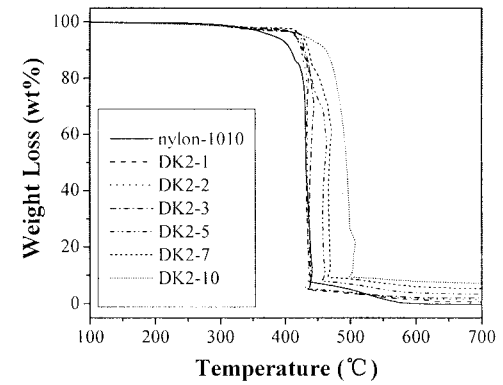

(a)

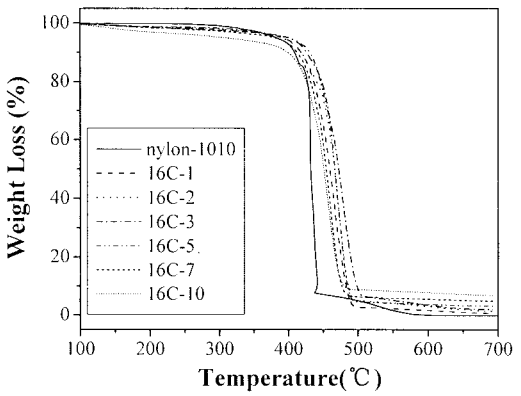

(b)

Figure 6 TGA curves of the nanocomposites: (a) the DK2-MMT nanocomposites with various DK2-MMT contents and (b) the 16C-MMT nanocomposites with different 16C-MMT contents.

are homogeneously dispersed in the nylon-1010 matrix and the space between the sheets is >10 nm. The micrograph confirms the formation of exfoliated morphology of the DK2-MMT nanocomposites. The orientation state of the DK2-MMT sheets in the matrix was probably caused during the process of injection molding. In Figure 4(b), 30–50 16C-MMT layers stack together, further demonstrating that the 16C-MMT nanocomposites form an intercalated structure.

Mechanical properties

The mechanical properties of the pure nylon-1010, the DK2-MMT nanocomposites, and the 16C-MMT nanocomposites are listed in Table I. As can be seen from Table I, the notched Izod impact strength of the DK2-MMT nanocomposites remains basically unchanged in the range of 1–3 wt % DK2-MMT content and then decreases above this range. For the 16C-MMT nanocomposites, the impact strength monotonously decreases with increasing 16C-MMT content. The poor impact property of the 16C-MMT nanocomposites is ascribed to the poor dispersion of 16C-MMT. The remaining mechanical properties of all the nanocomposites, regardless of the type of the fillers, increase with increased loading of the fillers. The enhancement of these properties can be attributed to the high aspect ratio of the organo-MMTs and interfacial interaction between the organo-MMTs and the nylon-1010 matrix. In addition, the mechanical properties of the DK2-MMT nanocomposites are superior to those of the 16C-MMT nanocomposites at the same filler content. For example, the tensile modulus of the DK2-MMT (3 wt %) nanocomposite and the 16C-MMT (3 wt %) nanocomposite is 1.97 GPa (a 36.8% increase) and 1.57 GPa (a 9.0% increase), respectively. The flexural strength of the two nanocomposites is 26.9% and 11.1% higher than that of the nylon-1010, respectively. The reason can be attributed to homogeneous dispersion of DK2-MMT in the nylon-1010 matrix.

Thermal stabilities

Figure 6(a) and (b) show TGA curves of the DK2-MMT nanocomposites and the 16C-MMT nanocomposites under air atmosphere, respectively. It is obvious that the addition of DK2-MMT into the nylon-1010 causes the TGA curves of the resulting nanocomposites to shift to higher temperature compared with the pure nylon-1010. Furthermore, the greater the content of DK2-MMT, the higher the temperature to which the

TABLE II
Thermal Properties of the DK2-MMT Nanocomposites

	MMT content												
	DK2-MMT (wt %)							16C-MMT (wt %)					
Property	0	1	2	3	5	7	10	1	2	3	5	7	10
T_i[a] (°C)	425.2	437.2	438.6	440.7	441.6	442.5	477.9	434.1	440.4	445.8	447.4	432.9	428.8
T_W[b] (°C)	381.4	415.4	414.7	422.3	417.1	425.7	427.9	390.6	389.1	398.9	399.1	378.8	305.8

[a] Initial decomposition temperature measured by TGA.
[b] Decomposition temperature at 5% weight loss determined by TGA.

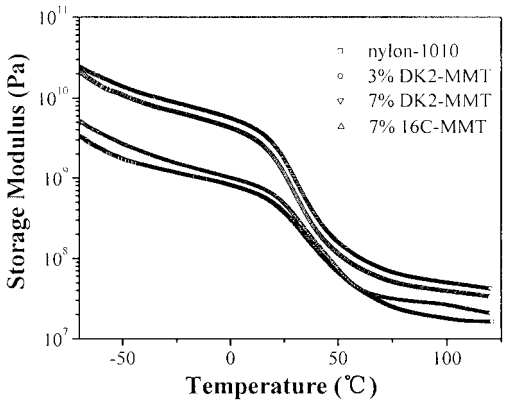

Figure 7 Temperature dependency of the storage modulus at 1 Hz for the nanocomposites.

TGA curves of the nanocomposites shift. When the DK2-MMT content is 10 wt %, the values of initial decomposition temperature (T_i) and decomposition temperature at a 5% weight loss (T_w) (Table II) of the nanocomposite are, respectively, 52.7 and 46.5°C higher than those of the pure nylon-1010. This indicates that the addition of DK2-MMT greatly improves the thermal stability of the nylon-1010 matrix. The improvement of thermal stability of the nanocomposites can be attributed to the barrier effect of MMT. MMT is a layered structure and small molecules generated during the thermal decomposition process cannot permeate, and thus have to bypass, MMT layers. Thus the addition of DK2-MMT slows down the decomposition of the nanocomposites. From Figure 6(b), the thermal stability of the nanocomposites is improved up to 7 wt % 16C-MMT, whereas the nanocomposite with 10 wt % 16C-MMT decomposed at a lower temperature relative to the pure nylon-1010. In addition, it can be found that all the 16C-MMT nanocomposites begin to lose weight at rather low temperature. From Table II, the T_i values of the 16C-MMT (≤7 wt %) nanocomposites are comparable to those of the DK2-MMT nanocomposites. However, the T_w value of the 16C-MMT (≤7 wt %) nanocomposites is obviously lower than that of the DK2-MMT nanocomposites. In the preparation of 16C-MMT, a portion of excessive hexadecyl trimethylammonium perhaps is absorbed on the surface of 16C-MMT and cannot be washed off. Absorbed hexadecyl trimethylammonium probably leads to slight enhancement of T_w and weight loss at low temperature of the 16C-MMT nanocomposites. Moreover, the decrease in thermal stability of the 16C-MMT (10 wt %) nanocomposite also can be explained through the above-mentioned analysis.

Dynamic mechanical properties of the nanocomposites

Figure 7 shows the temperature dependency of the storage modulus (E') for pure nylon-1010, the DK2-MMT nanocomposites with 3 and 7 wt % DK2-MMT content, and the 16C-MMT nanocomposite with 7 wt % 16C-MMT. As expected, E' of the nylon-1010 is greatly increased in the range of testing temperature when any one of the organo-MTTs is introduced. For example, E' values of the nanocomposites at −50°C and 100°C are listed in Table III: E' values at −50°C of the nanocomposite containing 3 and 7 wt % DK2-MMT are 1.53 and 7.91 times that of the pure nylon-1010, respectively. Meanwhile, it may be observed that the E' value of the DK2-MMT (7 wt %) nanocomposite is higher than that of the 16C-MMT (7 wt %) nanocomposite. The better dispersion of DK2-MMT in the nyon-1010 matrix may be the reason for the higher E' value of the DK2-MMT nanocomposite with respect to the 16C-MMT nanocomposite.

TABLE III
T_g and E' Values of the Samples

	MMT content (wt %)			
	DK2-MMT			16C-MMT
Property	0	3	7	7
T_g[a] (°C)	34.9	37.3	43.4	35.9
E'[b] (GPa)	1.76	2.70	13.92	10.85
E'[c] (GPa)	0.018	0.027	0.051	0.040

[a] Glass-transition temperature measured by DMA.
[b] Storage modulus measured by DMA at −50°C.
[c] Storage modulus measured by DMA at 100°C.

Figure 8 shows the temperature dependency of tan δ for the nanocomposites. The tan δ peaks correspond to the glass transition of the nylon-1010 and the nanocomposites, which are caused by the movement of chain segments of nylon-1010 amorphous chains. Glass-transition temperatures (T_g) of the samples are listed in Table III. It may be observed that the T_g values of the nanocomposites shift to a slightly higher temperature compared to that of the nylon-1010. Li-

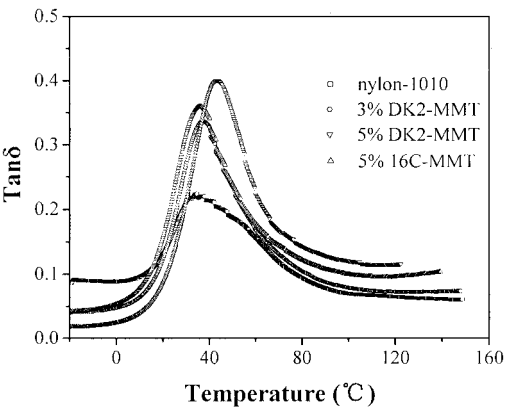

Figure 8 Temperature dependencies of tan δ at 1 Hz for the nanocomposites.

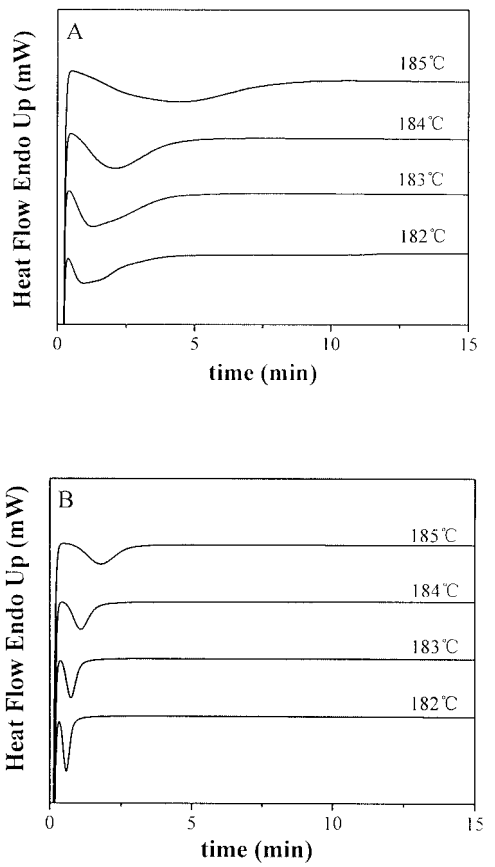

Figure 9 DSC thermograms of isothermal crystallization for (A) the nylon-1010 and (B) the DK2-MMT (3 wt %) nanocomposite.

ang et al.[18] also found a similar phenomenon that the addition of MMT to polyimide (PI) caused an increase of T_g of the PI. They attributed this phenomenon to the strong interaction between the MMT and the PI matrix, which constrains the movement of the PI chain segments.

Isothermal crystallization kinetics of the DK2-MMT (3 wt %) nanocomposite

As a sort of exterior impurities, nanoscale MMT layers can inevitably affect the crystallization behaviors of nylon-1010 (a semicrystalline polymer). Therefore, the isothermal crystallization kinetics of the DK2-MMT (3 wt %) nanocomposite was investigated. The DSC thermograms of isothermal crystallization of the nylon-1010 and the DK2-MMT (3 wt %) nanocomposite at different temperature are presented in Figure 9. As shown in Figure 9, with increasing crystallization temperature, a longer time was needed to complete the crystallization for both the nylon-1010 and the nylon-1010/DK2-MMT nanocomposite. One can find that $\tau_{1/2}$ (the half-time of crystallization; Table IV) of the DK2-MMT nanocomposite dramatically shortens compared with that of the pure nylon-1010, implying that the introduction of DK2-MMT substantially accelerates the crystallization rate of the nylon-1010 matrix.

The well-known Avrami equation[19,20] is the most commonly used approach to study the isothermal crystallization process of polymers:

$$X_t = 1 - \exp(Z_t t^n) \quad (1)$$

where n is the Avrami exponent and contains information on nucleation and crystal growth, Z_t is the Avrami rate constant, and X_t is the relative crystallinity at time t. Using eq. (1) in double-logarithmic form

$$\log[-\ln(1 - X_t)] = \log Z_t + n \log t \quad (2)$$

and plotting $\log[-\ln(1 - X_t)]$ against $\log t$, a straight line is obtained, and $\log Z_t$ and n can be estimated by linearly fitting this straight line. Plots of $\log[-\ln(1 - X_t)]$ versus $\log t$ for isothermal crystallization of the two samples are shown in Figure 10. The plots possess good linearity in a wide relative crystallinity range. It means that the Avrami equation can be successfully used to analyze the isothermal crystallization process. The Avrami exponent n and the Avrami rate constant Z_t can be obtained from the values of the slope and intercept of the fitted straight lines. The values of Z_t and n are listed in Table IV. The change of Z_t value before and after the addition of DK2-MMT also suggests the accelerating action of DK2-MMT on the crystallization of the nylon-1010 matrix. The n value is 1.76–2.37 for the nylon-1010 and 2.55–2.75 for the DK2-MMT nanocomposite, respectively. The difference in n values for the two samples indicates that DK2-MMT influences the crystallization behaviors of the nylon-1010 matrix.

CONCLUSIONS

The DK2-MMT nanocomposites and the 16C-MMT nanocomposites were successfully synthesized by melt intercalation. The difference in the properties of

TABLE IV
Isothermal Crystallization Kinetics Parameters of Nylon-1010 and the DK2-MMT (3 wt %) Nanocomposite

Sample	DK2-MMT content (wt %)	T_c (°C)	Z_t	n	$\tau_{1/2}$ (min)
Nylon-1010	0	182	0.59	1.76	1.03
		183	0.30	2.01	1.41
		184	0.13	2.37	1.84
		185	0.03	2.27	3.87
Nylon-1010	3	182	23.4	2.75	0.25
		183	7.24	2.55	0.41
		184	1.74	2.64	0.67
		185	0.34	2.71	1.27

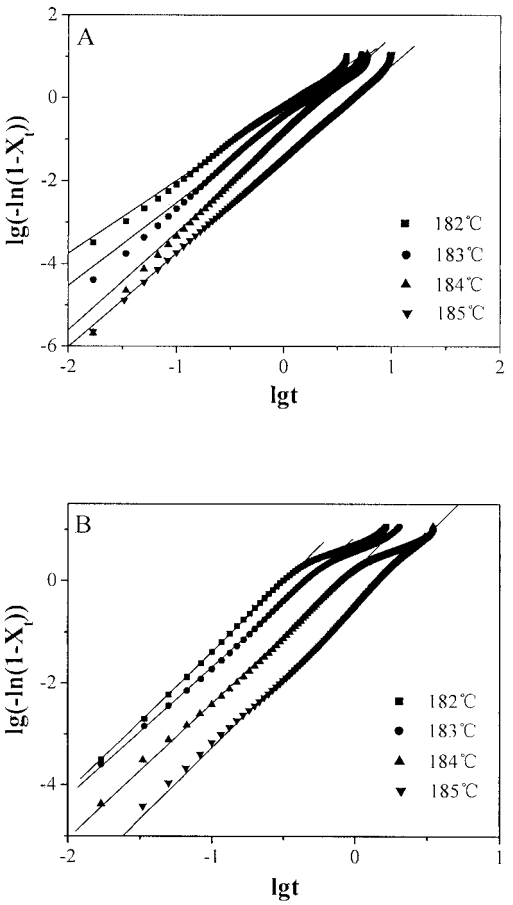

Figure 10 Plots of $\log[-\ln(1 - X_t)]$ versus $\log t$ for isothermal crystallization of (A) the nylon-1010 and (B) the DK2-MMT (3 wt %) nanocomposite.

the two types of the organo-MMTs directly influences the structure and the properties of the obtained nanocomposites. X-ray diffraction analysis and transmission electron microscope images show that the former form an exfoliated or partially exfoliated structure and the latter are characterized by an intercalated structure. The mechanical properties of all the nanocomposites are substantially improved because of the nanoscale dispersion of the organo-MMTs in the nylon-1010 matrix. Furthermore, because of the better dispersion of DK2-MMT, the DK2-MMT nanocomposites possess more excellent mechanical properties than those of the 16C-MMT nanocomposites. The thermal decomposition temperature of all the nanocomposites is higher than that of the pure nylon-1010. The E' value of the two types of the nanocomposites dramatically increased and the T_g shifted to higher temperature relative to that of the pure nylon-1010. In addition, the study of isothermal crystallization kinetics on the DK2-MMT nanocomposite suggests that the introduction of DK2-MMT accelerates the crystallization of nanocomposites and changes the crystallization behaviors of the nanocomposite.

The authors thank the Ministry of Science and Technology of China (973 Project No. G1999064802) for its financial support.

References

1. Kojima, Y.; Usuki, A.; Kawasumi, M.; Okada, A.; Kurauchi, T.; Kamigaito, O. J Polym Sci Part A: Polym Chem 1993, 31, 983.
2. Kojima, Y.; Usuki, A.; Kawasumi, M.; Okada, A.; Kurauchi, T.; Kamigaito, O. J Polym Sci Part A: Polym Chem 1993, 31, 1755.
3. Burnside, S. D.; Giannelis, E. P. J Polym Sci Part B: Polym Phys 2000, 38, 1595.
4. Kurokawa, Y.; Yasuda, H.; Oya, A. J Mater Sci Lett 1996, 15, 1481.
5. Kawasumi, M.; Hasegawa, N.; Kato, M.; Usuki, A.; Okada, A. Macromolecules 1997, 30, 6333.
6. Hasegawa, N.; Kawasumi, M.; Kato, M.; Usuki, A.; Okada, A. J Appl Polym Sci 1998, 67, 87.
7. Zhang, Q.; Fu, Q.; Jiang, L. X.; Lei, Y. Polym Int 2000, 49, 1561.
8. Sun, T.; Garces, J. M. Adv Mater 2002, 14, 128.
9. Doh, J. G.; Cho, I. Polym Bull 1998, 41, 511.
10. Zhu, J.; Morgan, A. B.; Lamelas, F. J.; Wilkie, C. A. Chem Mater 2001, 13, 3774.
11. Agag, T.; Koga, T.; Takeichi, T. Polymer 2001, 42, 3399.
12. Chang, J. H.; Park, K. M. Polym Eng Sci 2001, 41, 2226.
13. Chin, I. J.; Thurn-Albrecht, T.; Kim, H. C.; Russell, T. P.; Wang, J. Polymer 2001, 42, 5947.
14. Salahuddin, N.; Moet, A.; Hiltner, A.; Baer, E. Eur Polym Mater 2002, 38, 1477.
15. Huang, X. Y.; Lewis, S.; Brittain, W. J. Macromolecules 2000, 33, 2000.
16. Lee, D. C.; Jang, L. W. J Appl Polym Sci 1996, 61, 1117.
17. Chen, H.; Yao, K.; Tai, J. J Appl Polym Sci 1999; 73, 425.
18. Liang, Z.-M.; Yin, J.; Xu, H.-J. Polymer 2003, 44, 1391.
19. Avrami, M. J Chem Phys 1939, 7, 1103.
20. Avrami, M. J Chem Phys 1940, 8, 212.